The Developmental Testbed Center's Report on the Inter-comparison of the New Surface Drag Parameterization schemes using WRFv3.4.1

Point of Contact: Hongli Jiang
5 September 2013

Executive Summary

In recent versions of the Weather Research and Forecasting (WRF) model, two new surface drag parameterization options, both associated with the Yonsei University (YSU) planetary boundary layer (PBL) scheme, have been developed to address the widely acknowledged high surface wind speed bias, especially over plains and valleys. The Developmental Testbed Center (DTC) has performed extensive testing of three WRF model configurations with the Advanced Research WRF (ARW) core in order to evaluate the performance of the new options. The baseline configuration utilized the physics suite being run in the ARW High-Resolution Window (HIRESW) forecast system run operationally at the National Centers for Environmental Prediction (NCEP). The two comparative configurations tested the effects of the surface drag parameterization scheme namelist option, *topo_wind*, which aims to correct the high wind bias seen in WRF. One configuration was run with *topo_wind=1* (TWIND1), which is based on the concept of a momentum sink term and makes use of the standard deviation of the subgrid-scale orography as well as the Laplacian of the topographic field. The second configuration was run with *topo_wind=2* (TWIND2), which determines the subgrid terrain variance and makes the surface drag, or roughness, used in the model dependent on it; also included is additional consideration for stability and wind speed. The baseline configuration had *topo_wind=0* (REF). These runs were cold start cases initialized every 36 hours and run out to 48 hours for one full year. This report summarizes the differences between the REF and TWIND1 configurations, and the REF and TWIND2 configurations. Focus will be on the standard verification metrics, including an assessment of the statistical significance (SS) and practical significance (PS). Bias-corrected root-mean-square-error (BCRMSE) and bias for temperature, dew point temperature and wind speed were evaluated but presented for surface variables only since the differences in the upper air results were frequently not SS. Very few SS pair-wise differences were noted in evaluation of 3-hourly and daily quantitative precipitation forecasts (QPF), and thus no Gilbert Skill Score (GSS) or frequency bias will be presented in this report. The following points summarize the SS and PS differences seen in the verification results between REF – TWIND1 and REF – TWIND2:

- Surface temperature
  - **BCRMSE**:

    PS pair-wise differences occur during the fall and winter seasons, typically in the overnight hours; all favor the REF configuration.

- **Bias**:
  Regardless of initialization time, a number of PS pair-wise differences favoring the REF configuration are noted during the overnight hours, most notably for the annual, fall and winter aggregations when comparing REF – TWIND1 and for all temporal aggregations for the REF – TWIND2 comparison.

- Surface dew point temperature
  - **BCRMSE**:
    For both initializations, a majority of SS pair-wise differences favor TWIND1/TWIND2; however, SS differences favoring REF are seen at longer forecast lead times for the 00 UTC initializations mostly during the winter and fall aggregations. No differences are PS.
  - **Bias:**
    A majority of the SS pair-wise differences favor the TWIND1/TWIND2 configuration, especially during the overnight hours. PS pair-wise differences are predominantly noted in the fall and winter aggregations and are generally seen at the longer forecast lead times, with no distinct signal in which configuration is favored.

- Surface wind speed
  - **BCRMSE**:
    For REF – TWIND1, a majority of forecast lead times are SS and favor the REF configuration for all temporal aggregations except summer, which exhibits the fewest SS pair-wise differences. No PS differences are noted.

    For REF – TWIND2, several SS pair-wise differences are noted, with TWIND2 favored more frequently for the summer aggregation and REF for the other temporal aggregations. None are PS.

  - **Bias**:
    For both initializations and all temporal aggregations, all forecast lead times are SS with a majority of the differences being PS. TWIND1/TWIND2 is favored for overnight hours (i.e., 03 – 15 UTC) and REF is favored for day time hours (i.e., 18 – 00 UTC). TWIND1/TWIND2 has more PS pair-wise differences in the fall and winter aggregations than during the other temporal aggregations.

1. Introduction

It is widely acknowledged that the Weather Research and Forecasting (WRF) model has a high surface wind speed bias, especially over plains and valleys (e.g., Bernardet et al. 2005; Roux et al. 2009; Mass and Ovens 2010, 2011). In recent versions of WRF, two new surface drag parameterization options, both associated with the Yonsei University (YSU) planetary boundary layer (PBL) scheme, have been developed. The Developmental Testbed Center (DTC) has performed testing and evaluation of three WRF model configurations with the Advanced Research WRF (ARW) core (Skamarock et al. 2008). The baseline configuration utilized the physics suite being run in the ARW High-Resolution Window (HIRESW) forecast system run operationally at the National Centers for Environmental Prediction (NCEP). The two comparative configurations tested the effects of the surface drag parameterization scheme namelist option, *topo_wind*, which aims to correct the high wind bias seen in WRF. One configuration was run with *topo_wind=1* (TWIND1; Jimenez and Dudhia 2011), which is based on the concept of a momentum sink term and makes use of the standard deviation of the subgrid-scale orography as well as the Laplacian of the topographic field. The second configuration was run with *topo_wind=2* (TWIND2; Mass and Ovens 2012), which determines the subgrid terrain variance and makes the surface drag, or roughness, used in the model dependent on it; also included is additional consideration for stability and wind speed. The baseline configuration had *topo_wind=0* (turned off, default). These runs were cold start cases initialized every 36 hours and run out to 48 hours for one full year.

2. Experiment Design

The end-to-end forecast system was composed of the WRF Preprocessing System (WPS), WRF, and the Unified Postprocessor (UPP). Post-processed forecasts were verified using the Model Evaluation Tools (MET), and NCAR Command Language (NCL) was used for graphics generation. In addition, the full data set was archived and is available for dissemination to the user community. The codes used were based on the official released versions of WPS (v3.4.1) and UPP (v2.0). The addition of the *topo_wind=2* option was not available in the WRF source code until the fall of 2012, after the release of WRFv3.4.1. Thus, a tag from the WRF repository, dated 11 November 2012 (v3.4.1+) will be used for this test.

2.1 Forecast Period

Forecasts were initialized every 36 hours from 1 July 2011 through 30 June 2012, consequently creating a default of initialization times including both 00 and 12 UTC, for a total of 244 cases (see Appendix A for a list of the cases). The forecasts were run out to 48 hours with output files generated every 3 hours.

The table below lists the forecast initializations that failed to complete the end-to-end process; the missing data and reason for failure is described in the table. All missing forecasts were due to missing or bad input data sets, not model crashes. A total of 232 cases ran to completion and were used in the verification results.

Missing forecasts:

Affected Cycles	Missing data	Reason
2011071712	wrf output	missing SST input data
2011080112	wrf output	missing SST input data
2011082400	wrf output	missing SST input data
2011121712	wrf output	missing GFS input data
2012011012	wrf output	missing GFS input data
2012011612	wrf output	missing GFS input data
2012012212	wrf output	missing GFS input data
2012042000	wrf output	missing GFS input data
2012042412	wrf output	missing GFS input data
2012042600	wrf output	missing GFS input data
2012050500	wrf output	missing GFS input data
2012060400	wrf output	missing SST input data

2.2 Initial and Boundary Conditions

Initial conditions (ICs) and lateral boundary conditions (LBCs) were derived from the 0.5° x 0.5° Global Forecast System (GFS). A daily, real-time sea surface temperature product from Fleet Numerical Meteorology and Oceanography Center (FNMOC) was used to initialize the sea surface temperature (SST) field for the forecasts.

The time-invariant components of the lower boundary conditions (topography, soil and vegetation type etc.) were derived from United States Geological Survey (USGS) input data and were generated through the *geogrid* program of WPS.

2.3 Model Configuration Specifics

2.3.1 Domain Configuration

A 15-km North American/5-km contiguous United States CONUS 2-way nested (*feedback=1*) domain was employed for this test (Fig. 1). The parent domain was positioned to minimize effects of lateral boundary condition propagation into the area of interest. The inner domain was defined to limit the impacts of complex terrain at the boundaries and covers the CONUS region in order to capture complex terrain, plains and coastal regions spanning from the Gulf of Mexico, north, to Central Canada. The outer domain has 656 x 464 gridpoints, for a total of 304,384 gridpoints, while the inner domain has 1048 x 748, for a total of 783,904 gridpoints. The Lambert-Conformal map projection was used and the model was configured to have 36 vertical levels (37 sigma entries), with a pressure top of 50 hPa.

2.3.2 Other Aspects of Model Configuration

The table below lists the physics suite configurations that were used in this testing. The configuration which set *topo_wind=0* will be referred to as REF, the configuration with

topo_wind=1 will be referred to as TWIND1, and the configuration with *topo_wind=2* will be referred to as TWIND2 in this report.

Table 1. Physics suite combinations for the surface drag parameterization sensitivity test.

	REF	TWIND1	TWIND2
Microphysics	Single-Moment 3 class	Single-Moment 3 class	Single-Moment 3 class
Radiation SW and LW	Dudhia/RRTM	Dudhia/RRTM	Dudhia/RRTM
Surface Layer	Monin-Obukhov similarity theory	Monin-Obukhov similarity theory	Monin-Obukhov similarity theory
Land-Surface Model	Unified Noah	Unified Noah	Unified Noah
PBL	YSU (*topo_wind=0*)	YSU (*topo_wind=1*)	YSU (*topo_wind=2*)
Convection	Kain-Fritsch scheme (d01 only)	Kain-Fritsch scheme (d01 only)	Kain-Fritsch scheme (d01 only)

A long timestep of 72 s and an acoustic step of 4 were used. Calls to the boundary layer, and microphysics were performed every time step, whereas the cumulus parameterization was called every 5 minutes for the outer domain only; calls to radiation were done every 30 minutes.

The ARW solver offers a number of run-time options for the numerics, as well as various filter and damping options (Skamarock et al. 2008). The ARW was configured to use the following numeric options: 3rd-order Runge-Kutta time integration, 5th-order horizontal momentum and scalar advection, and 3rd-order vertical momentum and scalar advection. In addition, the following filter/damping options will be utilized: three-dimensional divergence damping (coefficient 0.1), external mode filter (coefficient 0.01), off-center integration of vertical momentum and geopotential equations (coefficient 0.1), vertical-velocity damping, and a 5-km-deep diffusive damping layer at the top of the domain (coefficient 0.01). Positive-definite moisture advection was also turned on.

2.4 Post-processing

The *unipost* program within UPP was used to destagger the forecasts, to generate derived meteorological variables, including mean sea level pressure, and to vertically interpolate fields to isobaric levels. The post-processed files included two- and three-dimensional fields on constant pressure levels, both of which were required by the plotting and verification programs.

Three-dimensional post-processed fields on model native vertical coordinates were also output and used to generate graphical forecast sounding plots.

The *copygb* program within UPP was used to interpolate the parent and nested domains to the same output grid over the CONUS domain at different resolutions.

3. Model Verification

The MET package was used to generate objective model verification. MET is comprised of grid-to-point verification, which was utilized to compare gridded surface and upper-air model data to point observations, as well as grid-to-grid verification, which was utilized to verify quantitative precipitation forecasts (QPF). Verification statistics generated by MET for each retrospective case were loaded into a MySQL database. Data was then retrieved from this database to compute and plot specified aggregated statistics using routines developed by the DTC in the statistical programming language, R.

Area-average results were computed for the parent (15-km; d01) and nested (5-km; d02) CONUS, CONUS-East, and CONUS-West domains, as well as the 14 sub-domains shown in Fig. 2. The focus for this report will be on verification results for surface variables over the CONUS domain with some brief discussions of the results from the sub-domains. Results for all verification domains are available on the DTC website (http://www.dtcenter.org/eval/meso_mod/topo_wind). In addition to the regional stratification, the verification statistics were also stratified by vertical level and lead time for the 00 UTC and 12 UTC initialization hours combined, and by forecast lead time and precipitation threshold for 00 UTC and 12 UTC initialized forecasts individually for surface fields in order to preserve the diurnal signal.

Each type of verification metric is accompanied by confidence intervals (CIs), at the 99% level, computed using the appropriate statistical method. All three configurations were run for the same cases allowing for a pair-wise difference methodology to be applied, as appropriate. The CIs on the pair-wise differences between statistics for two configurations objectively determines whether the differences are statistically significant (SS); if the CIs on the median pair-wise difference statistics include zero, the differences are not SS. Due to the nonlinear attributes of frequency bias, it is not amenable to a pair-wise difference comparison. Therefore, the more powerful method to establish SS could not be used and, thus, a more conservative estimate of SS was employed based solely on whether the aggregate statistics, with the accompanying CIs, overlapped between the two configurations. If no overlap was noted for a particular threshold, the differences between the two configurations were considered SS.

Due to the large number of cases used in this test, many SS pair-wise differences were anticipated. In many cases, the magnitude of the SS differences was quite small and did not yield practically meaningful results. Therefore, in addition to determining SS, the concept of establishing practical significance (PS) was also utilized for this test. PS was determined by filtering results to highlight pair-wise differences greater than the operational measurement uncertainty requirements and instrument performance as specified by the World Meteorological Organization (WMO;

http://www.wmo.int/pages/prog/gcos/documents/gruanmanuals/CIMO/CIMO_Guide-7th_Edition-2008.pdf). (Annex1.B). To establish PS between any two configurations, the following criteria were applied: temperature and dew point temperature differences greater than 0.1 K and wind speed differences greater than 0.5 m s^{-1}. PS was not considered for metrics used in precipitation verification [i.e., Gilbert Skill Score (GSS) or frequency bias] because those metrics are calculated via a contingency table, which is based on counts of yes and no forecasts.

3.1 Temperature, Dew Point Temperature, and Winds

Forecasts of surface and upper air temperature, dew point temperature, and wind were bilinearly interpolated to the location of the observations (METARs and RAOBS) within the NCEP North American Data Assimilation System (NDAS) prepbufr files. Objective model verification statistics were then generated for surface (using METAR) and upper air (using RAOBS) temperature, dew point temperature, and wind. Because shelter-level variables are not available from the model at the initial time, surface verification results start at the 3-hour lead time and go out 48 hours by 3-hour increments. For upper air, verification statistics were computed at the mandatory levels using radiosonde observations and computed at 12-hour intervals out to 48 hours. Because of known errors associated with radiosonde moisture measurements at high altitudes, the analysis of the upper air dew point temperature verification focuses on levels at and below 500 hPa. Bias and bias-corrected root-mean-square-error (BCRMSE) were computed separately for surface and upper air observations. The CIs were computed from the standard error estimates about the median value of the stratified results using a parametric method and a correction for first-order autocorrelation.

3.2 Precipitation

For the QPF verification, a grid-to-grid comparison was made by first bilinearly interpolating the precipitation analyses to the 15-km, and 5-km model integration domains, respectively. This regridded analysis was then used to evaluate the forecast. Accumulation periods of 3 and 24 hours were examined. NCEP Stage II analysis was used as the observational dataset, which is available in hourly, 6-hourly, and 24-hourly accumulations. For this test, hourly data was summed for the 3-hour QPF verification, and daily QPF verification utilized the 24-hour accumulation files. The 24-hour accumulation observations are valid at 12 UTC; therefore, the daily QPF was examined for the 24- and 48-hour lead times for the 12 UTC initializations and 36-hour lead time for the 00 UTC initializations. Traditional verification metrics computed included the GSS and frequency bias. For the precipitation statistics, a bootstrapping CI method was applied.

4. Verification Results

Pair-wise difference calculations were computed for REF – TWIND1 and REF – TWIND2. BCRMSE is always a positive quantity and a perfect score is zero. As a result, differences that are negative (positive) indicate the REF (TWIND1, TWIND2) configuration has a lower BCRMSE and is favored. Bias also has a perfect score of zero but can have positive or negative values; therefore, when looking at the pair-wise differences it is important to also note the magnitude and sign of the bias in relation to the perfect score for each individual

configuration to know which configuration has a smaller bias and is, thus, favored. In addition to time series plots, the surface verification statistics are also available by region.

For GSS, the perfect score is one and the no-skill score is zero. Thus, if the pair-wise difference is positive (negative), the REF (TWIND1, TWIND2) configuration has a higher GSS and is favored. For the frequency bias of QPF, a perfect score is one.

A breakdown of the configuration with SS (light shading) and PS (dark shading) better performance by variable, season, statistics metric, initialization hour, forecast lead time, and pressure level is summarized in Tables 2 - 7, where the favored configuration is highlighted. All verification plots generated (by plot type, metric, lead time, threshold, season, domain, etc.) can be viewed on the DTC Mesoscale Modeling testing and evaluation webpage (http://www.dtcenter.org/eval/meso_mod/topo_wind/verify/).

4.1 Upper air

Inter-comparisons of the REF – TWIND1 and REF – TWIND2 configurations, regardless of forecast lead time or temporal aggregation, show very few SS pair-wise differences in either bias or BCRMSE for all upper air variables. When SS pair-wise differences are noted, they are mainly located in the lowest vertical levels. Due to the small number of SS pair-wise differences, no results or comparisons of the different configurations for the vertical distributions will be discussed further in this report.

4.2 3-Hourly and Daily QPF GSS and bias

For all the configurations tested, regardless of initialization or forecast lead time, the 3-hourly and daily QPF GSS steadily decreases as the threshold increases. Only a few SS pair-wise differences are noted between the REF – TWIND1 and REF – TWIND2 inter-comparisons when considering 3-hourly and daily QPF GSS (not shown). No SS pair-wise differences are observed for the 3-hourly and daily QPF frequency bias (not shown). Due to the small number of SS pair-wise differences, no further discussion of the results for the different configurations will be presented in this report.

4.3 Surface

4.3.1 Temperature BCRMSE and Bias

4.3.1.1 REF, TWIND1, TWIND2

Regardless of the configuration examined, the surface temperature BCRMSE displays a general increase with lead time for both the 00 and 12 UTC initializations and for all temporal aggregations (Fig. 3). A diurnal signal is noted with the lowest BCRMSE values occurring at times valid at and around 15 – 18 UTC for 00 UTC initialization and all temporal aggregations.

In general, a cold bias in surface temperature is observed at all forecast lead times for both 00 and 12 UTC initializations (Fig. 4). The bias displays a strong diurnal modulation on top of a gentler trend of increasing bias (more negative) with lead time (smallest for the summer

aggregation). For all three configurations, both initializations, and all temporal aggregations, the cold bias magnitude is the largest around 00 UTC (i.e., during late afternoon) and smallest at 12 UTC (i.e., earlier morning). The amplitude of the diurnal cold bias signal is larger in the winter compared to the summer (i.e., warmer overnight and colder during the day).

Sub-domain verification of surface temperature shows a cold bias for most regions and lead times (Fig. 5), regardless of configuration examined. The only exception is a warm bias for two western regions (GRB and SWC) valid at 12 UTC. The cold bias is strongest at times valid at 00 UTC; it is most intense over the Rocky Mountain regions including GRB, SMT, and NMT, as well as APL, perhaps signaling a relationship to complex terrain. Relatively smaller magnitude cold biases are seen for the rest of the regions.

4.3.1.2 REF – TWIND1

While nearly all SS pair-wise differences noted for the surface temperature BCRMSE favor the REF configuration, the only PS differences occur during the winter and fall seasons, generally at times valid at and around 06 UTC (Table 2). All PS differences favor the REF configuration.

For surface temperature bias, a number of PS pair-wise differences favoring the REF configuration are noted during the overnight hours, especially for the annual, fall and winter seasons (Table 2). Several SS differences favoring TWIND1 are seen during the daytime hours for the spring and summer seasons, none of which are PS.

4.3.1.3 REF – TWIND2

Similar to REF – TWIND1, the only PS pair-wise differences for surface temperature BCRMSE occur during the fall and winter seasons, all of which favor the REF configuration (Table 3). The PS differences typically are seen in the overnight hours.

As compared to REF – TWIND1, more PS pair-wise differences are seen for the REF – TWIND2 temperature bias comparison, with a higher occurrence during the spring and summer aggregations. All PS pair-wise differences show REF as the better performer, with most differences generally seen for valid times between 00 and 15 UTC.

4.3.2 Dew Point Temperature

4.3.2.1 REF, TWIND1, TWIND2

Similar to surface temperature BCRMSE, an increase with lead time in dew point temperature BCRMSE is noted for both initializations and all temporal aggregations (Fig. 6). Diurnal variations are shown in all temporal aggregations (not shown) but are strongest in the annual, spring and summer, and the diurnal modulations are more pronounced for the 12 UTC initializations. In general, the largest BCRMSE values are seen for valid times around 21 – 00 UTC and the smallest during the overnight/early morning hours between 09 – 15 UTC.

A strong diurnal cycle is noted in the bias for both initializations and all temporal aggregations; the spring aggregation exhibits the largest amplitude, while winter, fall, and annual aggregations have a similar, but slightly smaller amplitude (Fig. 7, only spring and winter are shown). For the annual aggregation and 00 UTC initializations, a general wet bias is seen for forecasts valid between 18 – 03 UTC. The surface dew point bias minimum occurs around times valid at 12 UTC, with the sign of the bias dependent on the temporal aggregation and forecast lead time. When the cold bias in surface temperature is strongest the dew point temperature exhibits a large wet bias. For most temporal aggregations, as forecast lead times increases, median bias values trend lower leading to a lower wet bias during the late afternoon but larger dry bias during the overnight hours (e.g., median bias value at the 24-h forecast lead time has a larger bias than at the 48-h forecast lead time).

When examining the regional plots, at the 00 UTC valid time (wet bias regime on average), the largest wet bias is seen in SMT, SPL, and GRB (Fig. 8). At the 12 UTC valid times (trending towards dry bias regime on average), the largest dry biases are found over the East (i.e., APL and NEC), the western Coastal regions (i.e., NWC, SWC) and the northern Rocky Mountains (NMT).

4.3.2.2 REF – TWIND1

The differences between the REF – TWIND1 configurations are generally small for surface dew point temperature BCRMSE. There are a number of SS pair-wise differences that generally favor TWIND1, namely at the short-to-middle forecast lead times; however, no PS pair-wise differences are noted over the CONUS domain (see Table 4).

For surface dew point temperature bias pair-wise differences, there are a larger number of SS differences favoring TWIND1; however, when looking at PS pair-wise differences, the favored configuration depends on the forecast lead time (Table 4). PS pair-wise differences are predominantly in the fall and winter aggregations and at forecast lead times at and beyond 18-h; the 00 UTC initializations more often favor TWIND1, and the 12 UTC initializations more often favor the REF configuration.

4.3.2.3 REF – TWIND2

As with REF – TWIND1, a number of SS pair-wise differences favoring TWIND2 are noted for BCRMSE; however, over the CONUS domain, none are PS (Table 5). When SS pair-wise differences favor the REF configuration it is typically for the 00 UTC initializations at longer forecast lead times.

A small number of PS differences are seen in the bias for surface dew point temperature for the fall and winter aggregations. In general, differences are observed at the longer forecast lead times, with the favored configuration dependent on the forecast lead time (Table 5).

4.3.3 Surface wind speed

4.3.3.1 REF, TWIND1, TWIND2

For all three configurations and all temporal aggregations, the surface wind speed BCRMSE increases with forecast lead time (Fig. 9). Diurnal signals are clearly noted for both initializations in the annual, spring, and summer aggregations with the largest errors near 00 UTC and the smallest around 12 UTC. The diurnal signal is very weak in fall and winter aggregations (not shown).

Strong diurnal variations are noted for all three configurations, both initialization times and all temporal aggregations for wind speed bias (Fig. 10). A higher wind bias is typically seen in the forecasts for the overnight hours (03 – 12 UTC), and lower wind bias is seen during the daytime hours (15 – 21 UTC) for the CONUS verification domain. Apart from the diurnal trend, there is a shift of the bias toward negative values (low wind bias) for the West verification domain, and higher wind bias values for the East verification domain for all temporal aggregations (only spring aggregation is shown).

4.3.3.2 REF – TWIND1

Only SS pair-wise differences are noted for surface wind BCRMSE and nearly all of the differences favor the REF configuration. The summer aggregation has the fewest number of SS pair-wise differences. None of the pair-wise differences are PS (Table 6).

For wind speed bias, both initializations and all temporal aggregations have SS pair-wise differences at all forecast lead times and a majority of the pair-wise differences are PS. For both initializations, the TWIND1 configuration is favored for overnight hours (i.e., 03 – 15 UTC), and the REF configuration is favored for day time hours (i.e., 18 – 00 UTC). TWIND1 has more PS pair-wise differences in the fall and winter aggregations than in the other temporal aggregations.

4.3.3.3 REF – TWIND2

A number of SS pair-wise differences are noted for BCRMSE, with the TWIND2 configuration favored more frequently for the summer aggregation, and REF is favored more frequently for the other temporal aggregations (Table 7). However, no PS pair-wise differences are noted for BCRMSE.

Similar to REF – TWIND1, both initializations and all temporal aggregations have SS pair-wise differences at all forecast lead times, and a large number of PS pair-wise differences are noted. The favored configuration is dependent on the valid time, where the TWIND2 configuration is favored for overnight hours (i.e., 03 – 15 UTC), and the REF configuration is favored for day time hours (i.e., 18 – 00 UTC).

5. Summary

In this end-to-end sensitivity test, three WRF-ARW configurations were tested in order to evaluate the performance of the new surface drag parameterization scheme namelist option, *topo_wind*. The baseline configuration had *topo_wind=0* (REF); the first comparison configuration was run with *topo_wind=1* (TWIND1), and the second comparison configuration was run with *topo_wind=2* (TWIND2). Keeping the physics options and initialization datasets intact, all three configurations were run over an identical set of cases spanning one year.

Pair-wise differences were computed between the REF – TWIND1 configurations, and the REF – TWIND2 configurations for several verification metrics, and an assessment of SS and PS were completed. Overall, there were a significant number of SS pair-wise differences between the REF – TWIND1 configurations, and the REF – TWIND2 configurations, but most of them were not PS in terms of BCRMSE. On the other hand, a significant number of SS pair-wise differences between the REF and TWIND1 configurations, and the REF and TWIND2 configurations were PS in terms of bias. The favored configuration is highly dependent on the verification metric, temporal aggregation, initialization time, and forecast lead time. While a majority of the PS pair-wise differences for surface temperature bias indicated that the REF configuration out-performed both the TWIND1 and TWIND2 configurations, the signal was not as decisive for surface wind bias. The REF configuration was favored during the daytime hours; however, TWIND1 and TWIND2 did provide forecast improvement in during the overnight hours.

6. References

Bernardet, L.R., L. Nance, H.-Y. Chuang, A. Loughe, M. Demirtas, S. Koch, and R. Gall, 2005: The developmental testbed center winter forecasting experiment. Preprints, 21st Conf. on Weather Analysis and Forecasting/17th Conf. on Numerical Weather Prediction, Washington, DC, Amer. Meteor. Soc.,7.1. [Available online at http://ams.confex.com/ams/pdfpapers/94730.pdf

Jimenez, P. A., and J. Dudhia, 2011: Improving the Representation of Resolved and Unresolved Topographic Effects on Surface Wind in the WRF Model. *J. Appl Meteor. and Climo,* **51,** 300-315.

Mass, C., and D. Ovens, 2011: Fixing WRF's high speed wind bias: A new subgrid scale drag parameterization and the role of detailed verification. Preprints, 24th Conf. on Weather and Forecasting/20th Conf. on Numerical Weather Prediction, Seattle, WA, Amer. Meteor. Soc., 9B.6. [Available online at http://ams.confex.com/ams/91Annual/webprogram/Paper180011.html]

Mass, C. 2012: Improved Subgrid Drag of Hyper PBL/Vertical Resolution? Dealing with the Stable PBL Problems in WRF. *WRF Users' Workshop,* Boulder, CO. [Available online at:http://www.mmm.ucar.edu/wrf/users/workshops/WS2012/ppts/3.4.pdf]

Roux, G., Y. Liu, L. D. Monache, R.-S. Sheu, and T. T. Warner, 2009: Verification of high resolution WRF-RTFDDA surface forecasts over mountains and plains. Preprints, 2009 WRF Users' Workshop, Boulder, CO, NCAR. [Available online at http://www.mmm.ucar.edu/wrf/users/workshops/WS2009/abstracts/5B-05.pdf.]

Skamarock, W. C., J. B. Klemp, J. Dudhia, D. O. Gill, D. M. Barker, W. Wang and J. G. Powers, 2008: A Description of the Advanced Research WRF Version 3, NCAR Tech Note, NCAR/TN–475+STR, 113 pp.

Table 2. SS (light shading) and PS (dark shading) pair-wise differences for the REF and TWIND1 configurations (where the highlighted configuration is favored) for surface temperature BCRMSE and bias by season and forecast lead time for the 00 UTC and 12 UTC initializations separately over the 5 km CONUS verification domain.

Surface Temperature			f03	f06	f09	f12	f15	f18	f21	f24	f27	f30	f33	f36	f39	f42	f45	f48
BCRMSE	00 UTC Initializations	Annual	REF	REF	REF	REF	REF	REF	REF	REF	REF	REF	REF	REF	REF	REF	REF	REF
		Summer	REF	REF	REF	--	--	--	--	--	REF	REF	REF	--	--	REF	--	--
		Fall	REF *	REF *	REF *	REF *	--	REF	REF	REF	REF *	REF *	REF	REF	--	REF	REF	REF
		Winter	REF	REF *	REF	REF	REF	REF	REF	REF	REF	REF *	REF *	REF *	REF	REF	REF	REF *
		Spring	REF	REF	REF	--	REF	REF	--	TWIND1	--	--	REF	--	--	--	--	TWIND1
	12 UTC Initializations	Annual	--	REF	REF	--	REF	REF	REF	REF	REF	REF	REF	REF	REF	REF	REF	REF
		Summer	--	REF	REF	--	REF	REF	REF	--	--	--	--	--	--	--	--	--
		Fall	--	REF	REF	REF	REF *	REF *	REF *	REF	--	REF	REF	REF	REF *	REF *	REF *	REF *
		Winter	REF	--	--	REF	REF *	REF *	REF *	REF	REF	REF	REF	REF	REF *	REF	REF	REF
		Spring	--	--	--	TWIND1	REF	REF	REF	--	--	--	--	--	--	--	REF	--
Bias	00 UTC Initializations	Annual	REF *	REF *	REF *	REF *	REF	REF	REF	REF	REF	REF *	REF *	REF *	REF	REF	--	--
		Summer	REF *	REF *	REF *	REF	REF	REF	--	TWIND1	REF	REF	REF	--	TWIND1	--	TWIND1	TWIND1
		Fall	REF *	REF *	REF *	REF *	REF	REF	REF	REF *	REF *	REF *	REF *	REF *	REF *	REF	--	REF *
		Winter	REF *	REF *	REF *	REF *	REF *	REF	REF	REF *	REF *	REF *	REF *	REF *	REF *	REF	REF	REF *
		Spring	REF *	REF *	REF *	REF *	REF	REF	--	TWIND1	REF	REF *	REF *	REF	TWIND1	--	TWIND1	TWIND1
	12 UTC Initializations	Annual	REF	REF	REF	--	REF	REF *	REF *	REF *	--	--	--	--	REF	REF *	REF *	REF *
		Summer	REF	REF	--	TWIND1	REF	REF	REF	--	TWIND1	TWIND1	TWIND1	TWIND1	--	REF	REF	--
		Fall	REF *	REF	REF	REF	REF *	REF *	REF *	REF *	REF	REF	--	REF *	REF *	REF *	REF *	REF *
		Winter	REF	REF	REF	REF	REF *	REF *	REF *	REF *	REF	REF	REF	REF *	REF *	REF *	REF *	REF *
		Spring	REF	REF	--	TWIND1	REF	REF	REF *	--	TWIND1	TWIND1	TWIND1	TWIND1	--	REF	REF	--

Table 3. SS (light shading) and PS (dark shading) pair-wise differences for the REF and TWIND2 configurations (where the highlighted configuration is favored) for surface temperature BCRMSE and bias by season and forecast lead time for the 00 UTC and 12 UTC initializations separately over the 5 km CONUS verification domain.

Surface Temperature			f03	f06	f09	f12	f15	f18	f21	f24	f27	f30	f33	f36	f39	f42	f45	f48
BCRMSE	00 UTC Initializations	Annual	REF	REF	REF	REF	REF	REF	REF	REF	REF	REF	REF	REF	REF	REF	REF	REF
		Summer	REF	REF	REF	--	--	--	--	--	--	--	--	--	--	--	--	--
		Fall	REF *	REF *	REF *	REF	--	REF	--	REF	REF	REF	REF	REF	--	REF	REF	REF
		Winter	REF	REF	REF	REF	REF	REF	--	REF	REF *	REF *	REF *	REF *	REF	REF	REF	REF *
		Spring	REF	REF	REF	--	--	--	--	--	REF	REF	REF	--	--	--	--	--
	12 UTC Initializations	Annual	--	REF	REF	--	REF	REF	REF	REF	--	--	--	REF	REF	REF	REF	REF
		Summer	TWIND2	--	--	--	--	REF	--	--	TWIND2	TWIND2	--	--	--	--	--	--
		Fall	--	REF	REF	REF	REF *	REF *	REF *	REF	--	REF	--	REF	REF *	REF *	REF *	REF *
		Winter	REF	--	--	REF	REF *	REF *	REF	REF	REF	REF	--	REF	REF	REF	REF	REF
		Spring	--	--	--	TWIND2	--	REF	--	--	--	--	--	TWIND2	--	--	--	--
Bias	00 UTC Initializations	Annual	REF *	REF *	REF *	REF *	REF	REF	REF	REF	REF *	REF *	REF *	REF *	REF	REF	--	--
		Summer	REF *	REF *	REF *	REF *	REF	REF	--	--	REF	REF *	REF *	REF	--	--	TWIND2	TWIND2
		Fall	REF *	REF *	REF *	REF *	REF *	REF	REF	REF *	REF *	REF *	REF *	REF *	REF *	REF	--	REF *
		Winter	REF *	REF *	REF *	REF *	REF *	REF	REF	REF *	REF *	REF *	REF *	REF *	REF *	REF	REF	REF *
		Spring	REF *	REF *	REF *	REF *	REF	REF	--	TWIND2	REF *	REF *	REF *	REF	TWIND2	--	--	TWIND2
	12 UTC Initializations	Annual	REF	REF	REF	--	REF *	REF *	REF *	REF *	--	REF	--	--	REF *	REF *	REF *	REF *
		Summer	REF	REF	--	TWIND2	REF	REF *	REF *	REF	TWIND2	--	--	TWIND2	--	REF *	REF *	--
		Fall	REF *	REF	REF	REF *	REF *	REF *	REF *	REF *	REF *	REF	REF	REF *	REF *	REF *	REF *	REF *
		Winter	REF *	REF	REF	REF *	REF *	REF *	REF *	REF *	REF *	REF	REF	REF *	REF *	REF *	REF *	REF *
		Spring	REF	REF	REF	TWIND2	REF	REF *	REF *	REF	TWIND2	--	TWIND2	TWIND2	--	REF	REF *	--

Table 4. SS (light shading) and PS (dark shading) pair-wise differences for the REF and TWIND1 configurations (where the highlighted configuration is favored) for surface dew point temperature BCRMSE and bias by season and forecast lead time for the 00 UTC and 12 UTC initializations separately over the 5 km CONUS verification domain.

Surface Dew Point Temperature			f03	f06	f09	f12	f15	f18	f21	f24	f27	f30	f33	f36	f39	f42	f45	f48
BCRMSE	00 UTC Initializations	Annual	--	TWIND1	TWIND1	TWIND1	--	--	--	--	--	TWIND1	TWIND1	TWIND1	--	--	--	REF
		Summer	--	--	--	TWIND1	--	--	--	REF	--	TWIND1	TWIND1	TWIND1	TWIND1	TWIND1	--	REF
		Fall	--	TWIND1	--	--	--	--	--	--	--	TWIND1	--	--	REF	REF	REF	REF
		Winter	--	TWIND1	TWIND1	--	--	--	--	--	TWIND1	TWIND1	--	--	REF	--	--	REF
		Spring	--	TWIND1	TWIND1	TWIND1	--	--	TWIND1	--	--	TWIND1	TWIND1	TWIND1	--	--	--	--
	12 UTC Initializations	Annual	TWIND1	TWIND1	TWIND1	--	TWIND1	TWIND1	TWIND1	TWIND1	--	--	--	REF	--	TWIND1	TWIND1	--
		Summer	TWIND1	TWIND1	TWIND1	--	--	TWIND1	TWIND1	TWIND1	--	--	--	--	--	TWIND1	TWIND1	--
		Fall	--	TWIND1	--	--	--	TWIND1	TWIND1	--	--	--	--	REF	--	--	--	REF
		Winter	TWIND1	TWIND1	TWIND1	--	TWIND1	TWIND1	TWIND1	TWIND1	--	--	--	--	--	--	--	--
		Spring	TWIND1	TWIND1	TWIND1	--	--	TWIND1	TWIND1	TWIND1	--	--	TWIND1	--	TWIND1	TWIND1	TWIND1	TWIND1
Bias	00 UTC Initializations	Annual	--	--	TWIND1	REF	TWIND1	TWIND1	TWIND1	TWIND1	TWIND1	REF	REF	REF	REF	TWIND1	TWIND1	TWIND1
		Summer	--	TWIND1	--	TWIND1	TWIND1	TWIND1	TWIND1	--	--	REF	REF	--	REF	TWIND1	TWIND1	--
		Fall	--	TWIND1	TWIND1	REF	REF	TWIND1	TWIND1	TWIND1	TWIND1	TWIND1	TWIND1 *	REF *	REF	REF *	TWIND1	TWIND1
		Winter	--	--	TWIND1	TWIND1	TWIND1	TWIND1 *	TWIND1 *	TWIND1	TWIND1 *	TWIND1 *	TWIND1 *	REF *	REF *	TWIND1 *	TWIND1 *	TWIND1 *
		Spring	--	TWIND1	TWIND1	--	TWIND1	TWIND1	TWIND1 *	--	--	TWIND1	REF	REF	TWIND1	TWIND1	TWIND1 *	--
	12 UTC Initializations	Annual	TWIND1	TWIND1	TWIND1	--	--	TWIND1	REF	REF	REF	TWIND1	TWIND1	TWIND1	TWIND1	REF	REF	REF
		Summer	TWIND1	TWIND1	TWIND1	--	--	--	REF	--	TWIND1	TWIND1	TWIND1	--	--	REF	--	--
		Fall	--	TWIND1	TWIND1	TWIND1	TWIND1	TWIND1	TWIND1	TWIND1 *	REF *	TWIND1 *	TWIND1	TWIND1	REF *	REF *	REF *	REF *
		Winter	TWIND1	TWIND1	TWIND1	TWIND1	TWIND1	TWIND1	TWIND1 *	TWIND1 *	REF *	TWIND1 *	TWIND1 *	TWIND1	TWIND1 *	REF *	REF *	REF *
		Spring	TWIND1	TWIND1	TWIND1	--	--	--	REF	REF	TWIND1	TWIND1	TWIND1	--	--	--	REF	--

Table 5. SS (light shading) and PS (dark shading) pair-wise differences for the REF and TWIND2 configurations (where the highlighted configuration is favored) for surface dew point temperature BCRMSE and bias by season and forecast lead time for the 00 UTC and 12 UTC initializations separately over the 5 km CONUS verification domain.

Surface Dew Point Temperature			f03	f06	f09	f12	f15	f18	f21	f24	f27	f30	f33	f36	f39	f42	f45	f48
BCRMSE	00 UTC Initializations	Annual	--	TWIND2	TWIND2	TWIND2	TWIND2	TWIND2	--	--	TWIND2	TWIND2	TWIND2	TWIND2	--	--	--	--
		Summer	REF	--	TWIND2	TWIND2	--	TWIND2	--	--	--	TWIND2	TWIND2	TWIND2	--	TWIND2	TWIND2	--
		Fall	--	TWIND2	TWIND2	--	--	--	--	--	TWIND2	TWIND2	TWIND2	--	REF	REF	REF	--
		Winter	--	TWIND2	TWIND2	TWIND2	--	--	--	--	TWIND2	TWIND2	--	--	REF	REF	REF	REF
		Spring	--	TWIND2	TWIND2	TWIND2	--	--	TWIND2	--	--	TWIND2	TWIND2	TWIND2	--	TWIND2	--	--
	12 UTC Initializations	Annual	TWIND2	TWIND2	TWIND2	--	TWIND2	TWIND2	TWIND2	TWIND2	--	TWIND2	TWIND2	--	TWIND2	TWIND2	TWIND2	--
		Summer	--	TWIND2	TWIND2	--	--	TWIND2	TWIND2	TWIND2	TWIND2	TWIND2	TWIND2	--	--	TWIND2	TWIND2	TWIND2
		Fall	--	TWIND2	--	--	TWIND2	TWIND2	TWIND2	TWIND2	--	--	--	REF	--	--	--	--
		Winter	TWIND2	TWIND2	TWIND2	--	TWIND2	TWIND2	TWIND2	TWIND2	--	--	--	--	--	--	--	--
		Spring	TWIND2	TWIND2	TWIND2	TWIND2	--	TWIND2	TWIND2	TWIND2	TWIND2	TWIND2	TWIND2	TWIND2	TWIND2	TWIND2	TWIND2	TWIND2
Bias	00 UTC Initializations	Annual	REF	--	TWIND2	REF	TWIND2	TWIND2	TWIND2	TWIND2	--	TWIND2	REF	REF	REF	TWIND2	TWIND2	TWIND2
		Summer	REF	TWIND2	--	--	TWIND2	TWIND2	TWIND2	--	--	--	--	--	REF	TWIND2	TWIND2	--
		Fall	--	TWIND2	TWIND2	REF	REF	TWIND2	TWIND2	--	--	TWIND2	TWIND2	REF *	REF *	REF *	TWIND2	--
		Winter	--	--	TWIND2	TWIND2	TWIND2	TWIND2 *	TWIND2	--	TWIND2	TWIND2 *	REF *	REF *	REF *	TWIND2 *	TWIND2 *	TWIND2 *
		Spring	--	--	TWIND2	--	TWIND2	TWIND2	TWIND2	--	REF	--	REF	REF	TWIND2	TWIND2 *	TWIND2	--
	12 UTC Initializations	Annual	TWIND2	TWIND2	TWIND2	REF	REF	--	REF	REF	REF	TWIND2	TWIND2	--	TWIND2	REF	REF	REF
		Summer	TWIND2	TWIND2	TWIND2	REF	TWIND2	TWIND2	--	--	--	TWIND2	TWIND2	--	--	--	--	--
		Fall	--	TWIND2	TWIND2	--	TWIND2	TWIND2	TWIND2	TWIND2 *	REF	TWIND2	TWIND2	TWIND2	TWIND2	REF *	REF *	REF *
		Winter	TWIND2	TWIND2	TWIND2	--	--	--	TWIND2	TWIND2 *	REF *	TWIND2 *	TWIND2 *	TWIND2	TWIND2	REF *	REF *	REF *
		Spring	TWIND2	TWIND2	TWIND2	REF	REF	--	--	--	TWIND2	TWIND2	TWIND2	--	REF	--	--	--

Table 6. SS (light shading) and PS (dark shading) pair-wise differences for the REF and TWIND1 configurations (where the highlighted configuration is favored) for surface wind BCRMSE and bias by season and forecast lead time for the 00 UTC and 12 UTC initializations separately over the 5 km CONUS verification domain.

Surface Wind Speed			f03	f06	f09	f12	f15	f18	f21	f24	f27	f30	f33	f36	f39	f42	f45	f48
BCRMSE	00 UTC Initializations	Annual	REF	REF	REF	REF	REF	REF	REF	REF	REF	REF	REF	--	--	REF	REF	REF
		Summer	REF	--	--	--	--	--	--	--	REF	REF	--	TWIND1	--	--	--	--
		Fall	REF	REF	REF	REF	REF	REF	REF	REF	REF	REF	REF	REF	REF	REF	REF	REF
		Winter	REF	REF	REF	REF	REF	REF	REF	REF	REF	REF	REF	REF	REF	REF	REF	REF
		Spring	REF	REF	REF	--	REF	REF	REF	REF	REF	--	--	--	--	REF	--	REF
	12 UTC Initializations	Annual	REF	REF	REF	REF	REF	REF	REF	REF	REF	REF	REF	REF	REF	REF	REF	--
		Summer	--	--	--	--	--	--	--	--	--	--	--	--	REF	--	--	TWIND1
		Fall	REF	REF	REF	REF	REF	REF	REF	REF	REF	REF	REF	REF	REF	REF	REF	REF
		Winter	REF	REF	REF	REF	REF	REF	REF	REF	REF	REF	REF	REF	REF	REF	REF	--
		Spring	REF	REF	REF	REF	REF	REF	--	--	REF	REF	--	REF	REF	--	--	--
Bias	00 UTC Initializations	Annual	TWIND1 *	TWIND1	TWIND1	TWIND1	TWIND1 *	REF *	REF *	TWIND1 *	TWIND1 *	TWIND1 *	TWIND1	TWIND1 *	TWIND1 *	REF *	REF *	TWIND1 *
		Summer	TWIND1	TWIND1	TWIND1	TWIND1	REF	REF *	REF *	TWIND1 *	TWIND1	TWIND1	TWIND1	TWIND1	REF *	REF *	REF *	REF *
		Fall	TWIND1 *	TWIND1 *	TWIND1 *	TWIND1 *	TWIND1 *	REF *	REF *	TWIND1 *	TWIND1 *	TWIND1 *	TWIND1 *	TWIND1 *	TWIND1 *	TWIND1 *	REF *	TWIND1 *
		Winter	TWIND1 *	TWIND1 *	TWIND1 *	TWIND1 *	TWIND1 *	REF *	REF *	REF *	TWIND1 *	TWIND1 *	TWIND1 *	TWIND1 *	TWIND1 *	REF *	REF *	TWIND1 *
		Spring	TWIND1 *	TWIND1	TWIND1	TWIND1 *	REF *	REF *	REF *	REF *	TWIND1 *	TWIND1 *	TWIND1 *	TWIND1 *	REF *	REF *	REF *	REF *
	12 UTC Initializations	Annual	TWIND1 *	REF *	REF *	TWIND1 *	TWIND1 *	TWIND1	TWIND1	TWIND1	TWIND1 *	REF *	REF *	REF *	TWIND1 *	TWIND1	TWIND1	TWIND1
		Summer	REF *	REF *	REF *	TWIND1 *	TWIND1 *	TWIND1	TWIND1	TWIND1	TWIND1 *	REF *	REF *	REF *	TWIND1	TWIND1	TWIND1	TWIND1
		Fall	TWIND1 *	REF *	REF *	TWIND1 *	TWIND1 *	TWIND1 *	TWIND1 *	TWIND1 *	TWIND1 *	REF *	REF *	TWIND1 *	TWIND1 *	TWIND1 *	TWIND1 *	TWIND1 *
		Winter	TWIND1 *	REF *	REF *	REF *	TWIND1 *	TWIND1 *	TWIND1 *	TWIND1 *	TWIND1 *	REF *	REF *	REF *	TWIND1 *	TWIND1 *	TWIND1 *	TWIND1 *
		Spring	REF *	REF *	REF *	REF *	TWIND1 *	TWIND1	TWIND1	TWIND1 *	REF *	REF *	REF *	REF *	TWIND1 *	TWIND1	TWIND1	TWIND1 *

Table 7. SS (light shading) and PS (dark shading) pair-wise differences for the REF and TWIND2 configurations (where the highlighted configuration is favored) for surface wind BCRMSE and bias by season and forecast lead time for the 00 UTC and 12 UTC initializations separately over the 5 km CONUS verification domain.

Surface Wind Speed			f03	f06	f09	f12	f15	f18	f21	f24	f27	f30	f33	f36	f39	f42	f45	f48
BCRMSE	00 UTC Initializations	Annual	REF	--	--	--	TWIND2	TWIND2	--	REF	REF	REF	--	TWIND2	TWIND2	TWIND2	--	REF
		Summer	--	TWIND2	TWIND2	TWIND2	TWIND2	TWIND2	TWIND2	--	--	--	--	TWIND2	TWIND2	TWIND2	TWIND2	--
		Fall	REF	REF	REF	REF	--	--	--	REF	REF	REF	--	--	--	--	REF	--
		Winter	REF	REF	--	--	TWIND2	--	--	--	--	--	--	--	TWIND2	TWIND2	--	REF
		Spring	REF	REF	--	--	--	--	--	REF	REF	REF	--	TWIND2	--	--	--	--
	12 UTC Initializations	Annual	TWIND2	--	--	REF	REF	REF	--	--	TWIND2	TWIND2	TWIND2	REF	REF	--	--	TWIND2
		Summer	TWIND2	TWIND2	TWIND2	TWIND2	--	--	TWIND2	TWIND2	TWIND2	TWIND2	TWIND2	--	--	--	--	TWIND2
		Fall	--	--	--	REF	REF	REF	--	--	--	--	--	REF	--	--	REF	--
		Winter	--	--	--	REF	REF	REF	--	--	TWIND2	--	--	--	--	--	--	--
		Spring	--	--	--	REF	--	--	--	TWIND2	--	--	TWIND2	REF	REF	--	--	--
Bias	00 UTC Initializations	Annual	TWIND2 *	TWIND2 *	TWIND2 *	TWIND2 *	TWIND2 *	REF *	REF *	TWIND2 *	TWIND2 *	TWIND2 *	TWIND2 *	TWIND2 *	TWIND2 *	REF *	REF *	TWIND2 *
		Summer	TWIND2	TWIND2	TWIND2	TWIND2	REF *	REF *	REF *	REF *	TWIND2 *	TWIND2	TWIND2	TWIND2	REF *	REF *	REF *	REF *
		Fall	TWIND2 *	TWIND2 *	TWIND2 *	TWIND2 *	TWIND2 *	REF *	REF *	TWIND2 *	TWIND2 *	TWIND2 *	TWIND2 *	TWIND2 *	TWIND2 *	REF *	REF *	TWIND2 *
		Winter	TWIND2 *	TWIND2 *	TWIND2 *	TWIND2 *	TWIND2 *	REF *	REF *	REF *	TWIND2 *	TWIND2 *	TWIND2 *	TWIND2 *	TWIND2 *	REF *	REF *	TWIND2 *
		Spring	TWIND2 *	TWIND2 *	TWIND2	TWIND2 *	REF *	REF *	REF *	REF *	TWIND2 *	TWIND2 *	TWIND2 *	TWIND2 *	REF *	REF *	REF *	REF *
	12 UTC Initializations	Annual	TWIND2 *	REF *	REF *	REF *	TWIND2 *	TWIND2 *	TWIND2	TWIND2 *	TWIND2 *	REF *	REF *	REF *	TWIND2 *	TWIND2 *	TWIND2	TWIND2 *
		Summer	REF *	REF *	REF *	TWIND2 *	TWIND2	TWIND2	TWIND2	TWIND2	REF *	REF *	REF *	REF *	TWIND2	TWIND2	TWIND2	TWIND2
		Fall	TWIND2 *	REF *	REF *	TWIND2 *	TWIND2 *	TWIND2 *	TWIND2 *	TWIND2 *	TWIND2 *	REF *	REF *	TWIND2 *	TWIND2 *	TWIND2 *	TWIND2 *	TWIND2 *
		Winter	TWIND2 *	REF *	REF *	REF *	TWIND2 *	TWIND2 *	TWIND2 *	TWIND2 *	TWIND2 *	REF *	REF *	REF *	TWIND2 *	TWIND2 *	TWIND2 *	TWIND2 *
		Spring	REF *	REF *	REF *	REF *	TWIND2 *	TWIND2 *	TWIND2	TWIND2 *	REF *	REF *	REF *	REF *	TWIND2 *	TWIND2	TWIND2	TWIND2 *

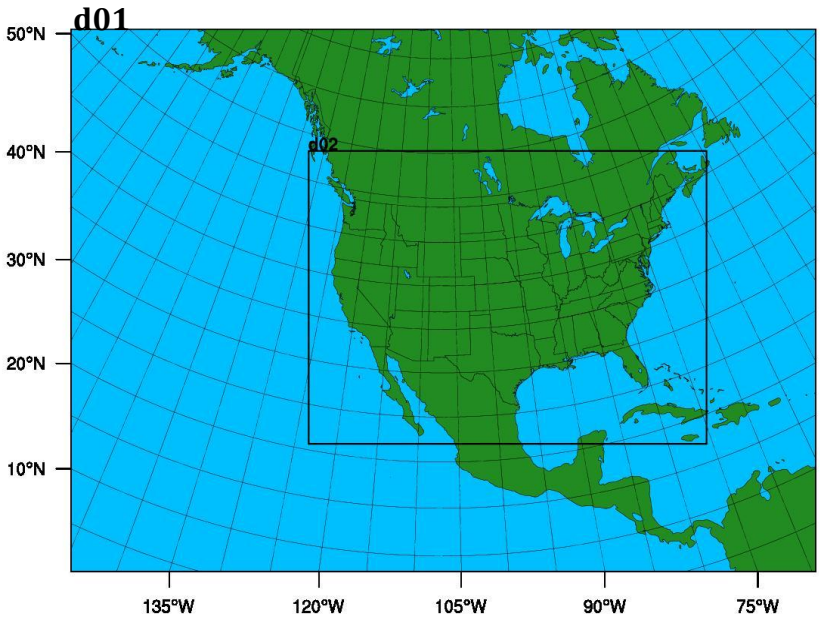

Figure 1. Map showing the boundary of the WRF-ARW computational domains.

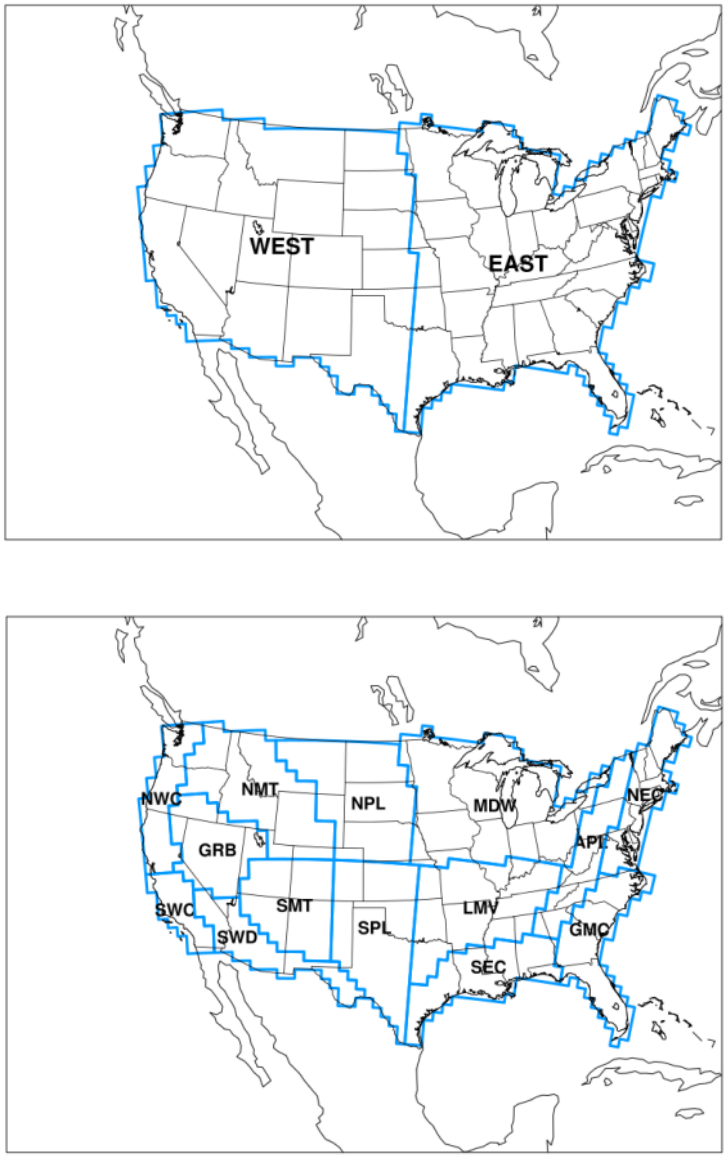

Figure 2. Map showing the locations of the CONUS-West, CONUS-East (top) and 14 regional verification domains (bottom). The outermost outline of the regional domains depicts the CONUS verification domain.

(a) Annual IH=00 UTC

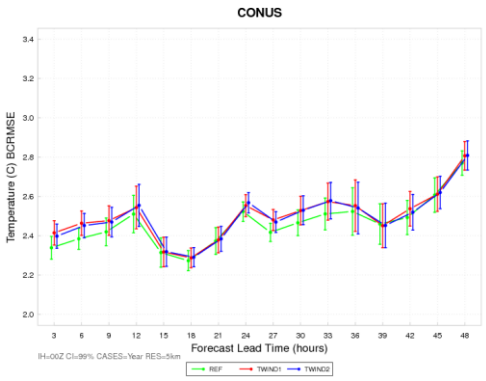

(b) Annual IH=12 UTC

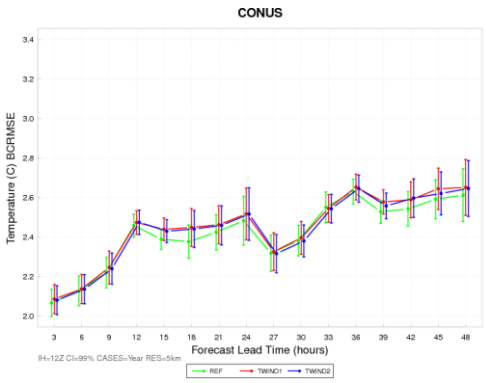

(c) Summer IH=00 UTC

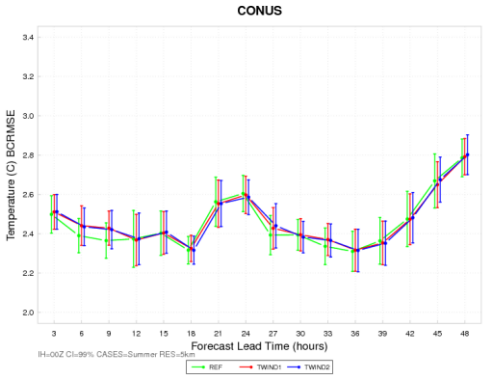

(d) Winter IH=00UTC

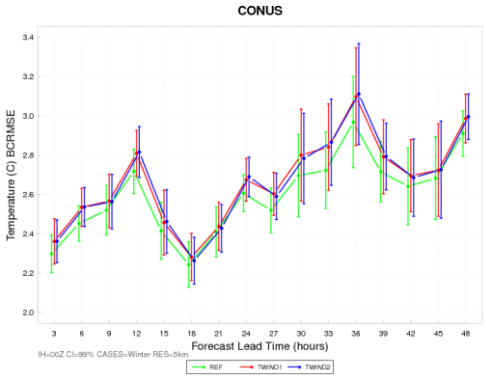

Figure 3. Time series plot of 2 m AGL temperature (°C) for median BCRMSE over the 5 km CONUS verification domain aggregated across the entire year of cases for the (a) 00 UTC initializations and (b) 12 UTC initializations and for the 00 UTC initializations for the (c) Summer aggregation and (d) Winter aggregation. The REF configuration is in green, the TWIND1 configuration in red, and the TWIND2 configuration in blue. The vertical bars attached to the median represent the 99% CIs.

(a) Annual IH=00 UTC

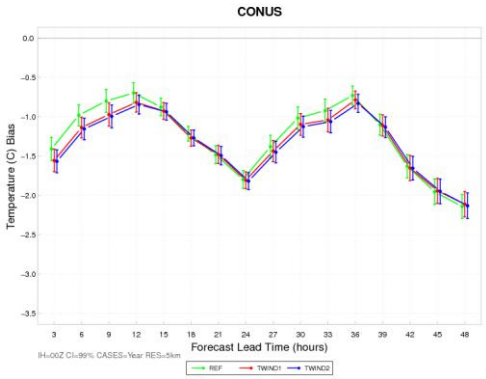

(b) Annual IH=12 UTC

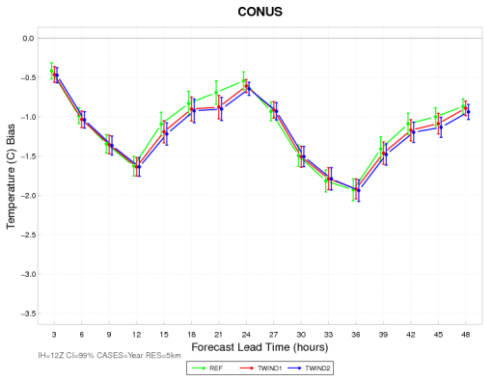

(c) Summer IH=00 UTC

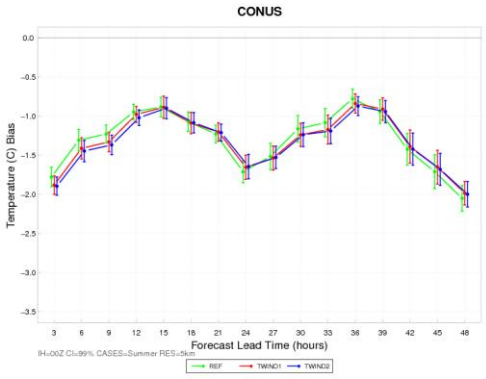

(d) Winter IH=00UTC

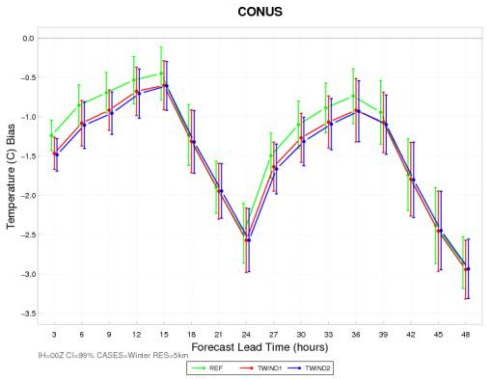

Figure 4. Time series plot of 2 m AGL temperature (°C) for median bias over the 5 km CONUS verification domain aggregated across the entire year of cases for the (a) 00 UTC initializations and (b) 12 UTC initializations and for the 00 UTC initializations for the (c) Summer aggregation and (d) Winter aggregation. The REF configuration is in green, the TWIND1 configuration in red, and the TWIND2 in blue. The vertical bars attached to the median represent the 99% CIs

(a) REF LT=24 h valid at 00 UTC

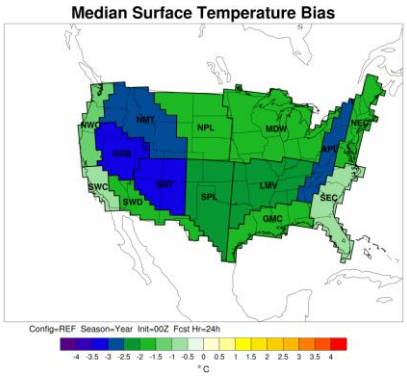

(b) REF LT=36 h valid at 12 UTC

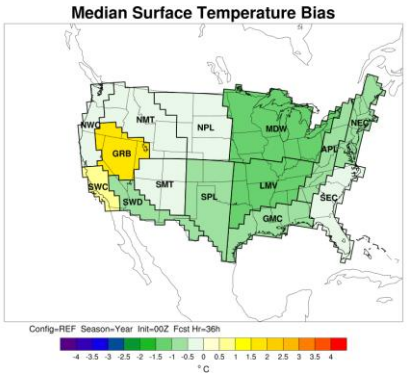

(c) TWIND1 LT=24 h valid at 00 UTC

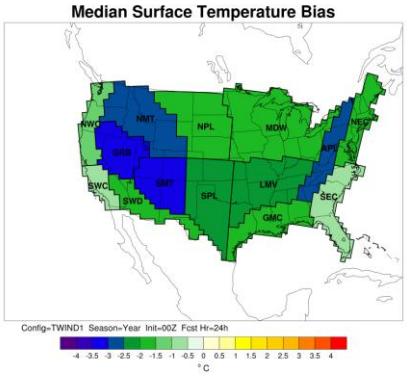

(d) TWIND1 LT=36 h valid at 12 UTC

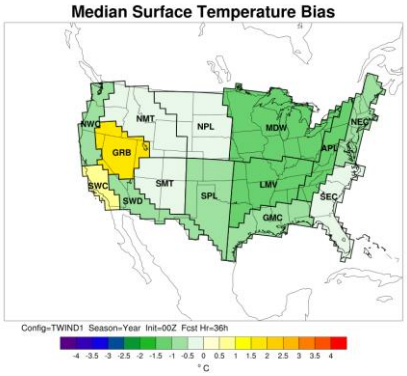

(e) TWIND2 LT=24 h valid at 00 UTC

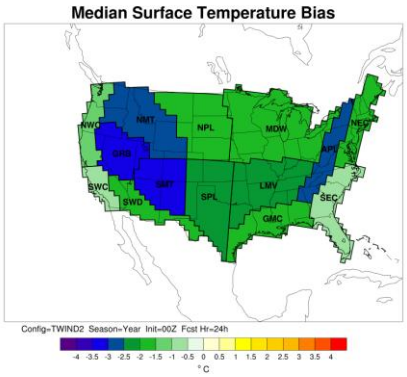

(f) TWIND2 LT=36 h valid at 12 UTC

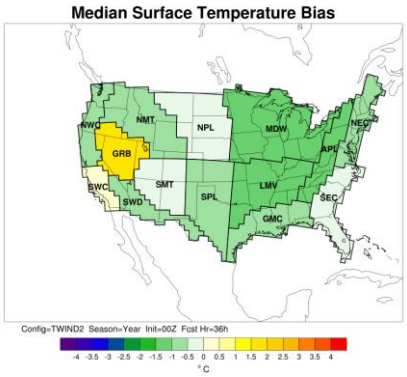

Figure 5. Regional median bias over the 5 km CONUS verification domain in 2 m AGL temperature (°C) for the 00 UTC initializations (a) the REF configuration at 24 h lead time, (b) the REF configuration at 36 h lead time, (c) the TWIND1 configuration at 24 h lead time, (d) the TWIND1 configuration at 36 h lead time, (e) the TWIND2 configuration at 24 h lead time, and (f) the TWIND2 configuration at 36 h lead time aggregated across the entire year of cases.

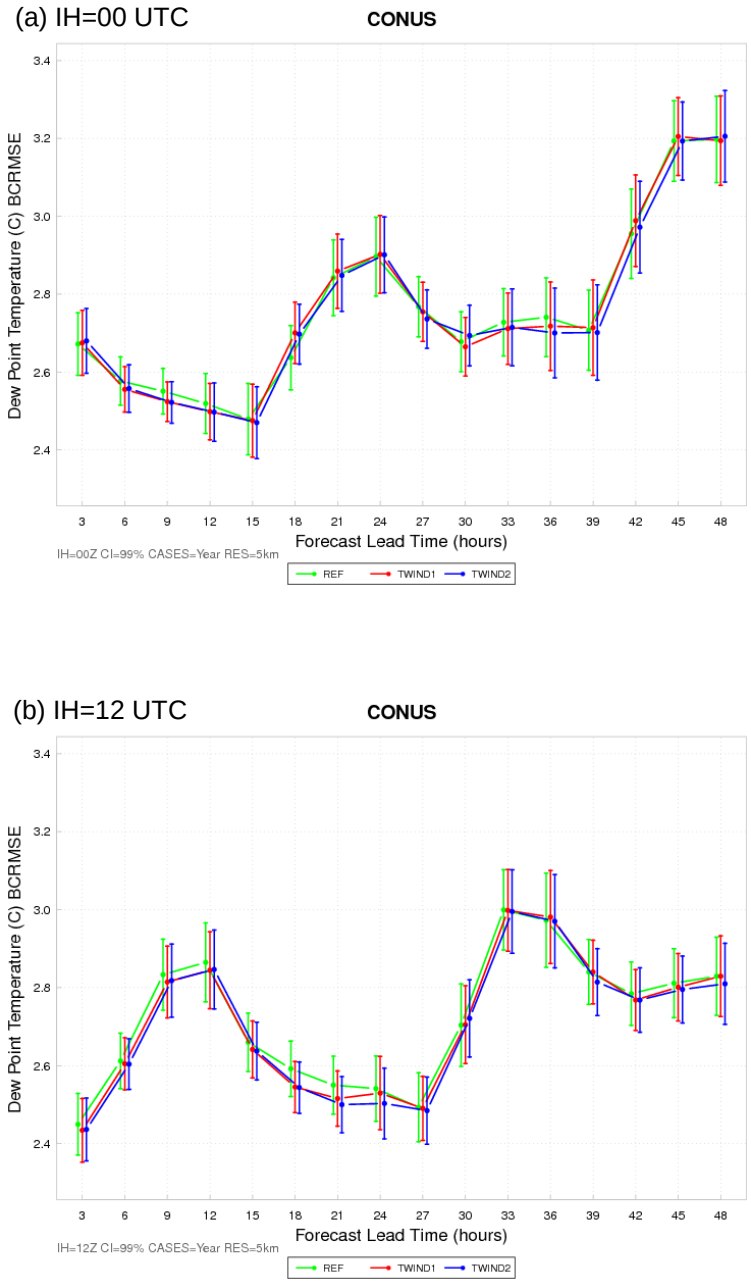

Figure 6. Time series plot of 2 m AGL dew point temperature (°C) for median BCRMSE over the 5 km CONUS verification domain for the (a) 00 UTC initializations and (b) 12 UTC initializations aggregated across the entire year of cases. The REF configuration is in green, the TWIND1 configuration in red, and the TWIND2 configurations in blue. The vertical bars attached to the median represent the 99% CIs.

(a) Annual IH=00 UTC

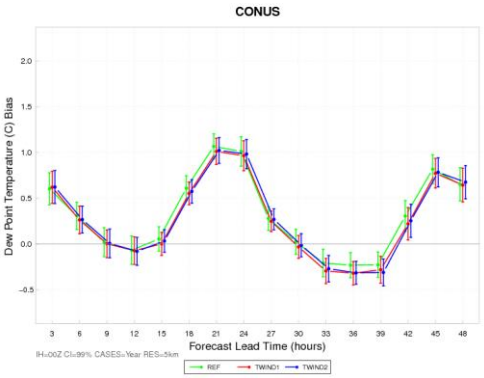

(b) Annual IH=12 UTC

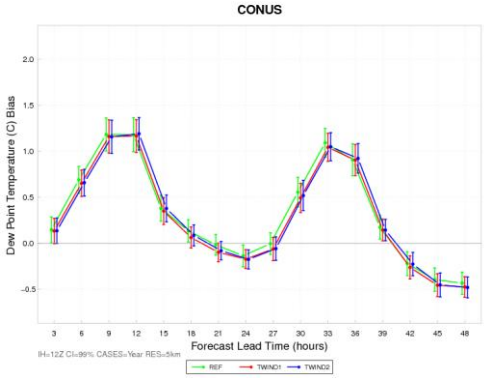

(c) Spring IH=00 UTC

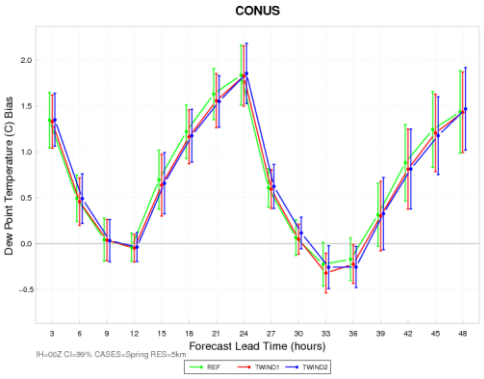

(d) Winter IH=00 UTC

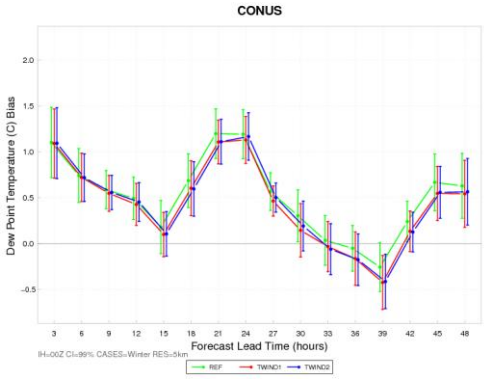

Figure 7. Time series plot of 2 m AGL dew point temperature (°C) for median bias over the 5 km CONUS verification domain aggregated across the entire year of cases for the (a) 00 UTC initializations, (b) 12 UTC initializations, (c) the spring aggregation, and (d) the winter aggregation for the 00 UTC initializations. The REF configuration is in green, the TWIND1 configuration in red, and the TWIND2 in blue. The vertical bars attached to the median represent the 99% CIs.

(a) REF LT=12 h valid at 00 UTC

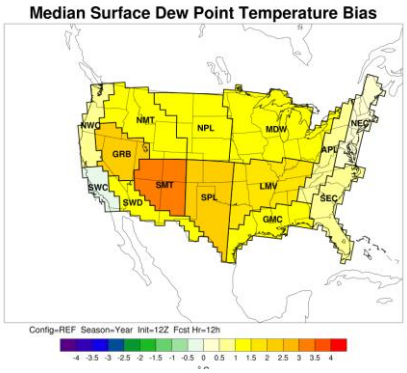

(b) REF LT=48 h valid at 12 UTC

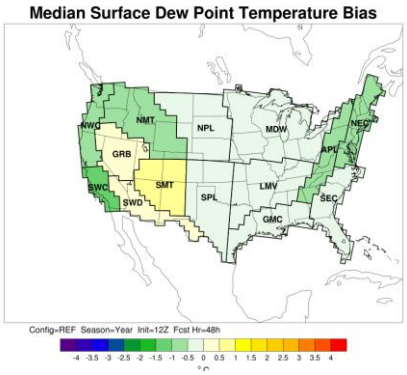

(c) TWIND1 LT=12 h valid at 00 UTC

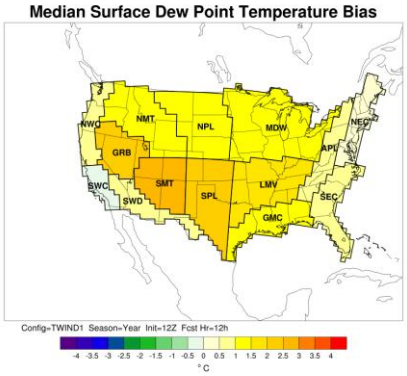

(d) TWIND1 LT=48 h valid at 12 UTC

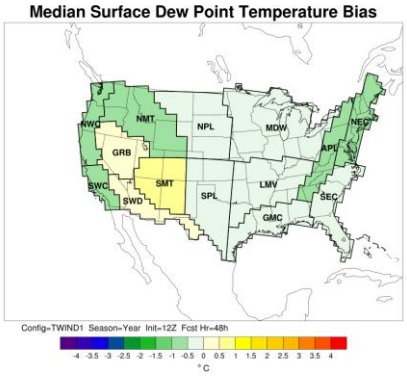

(e) TWIND2 LT=12 h valid at 00 UTC

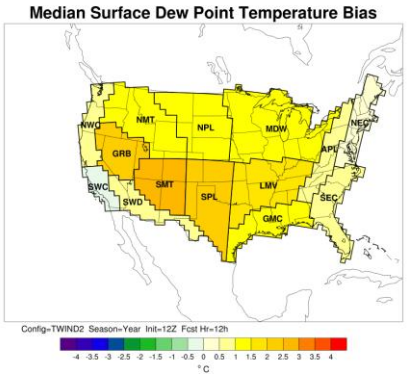

(f) TWIND2 LT=48 h valid at 12 UTC

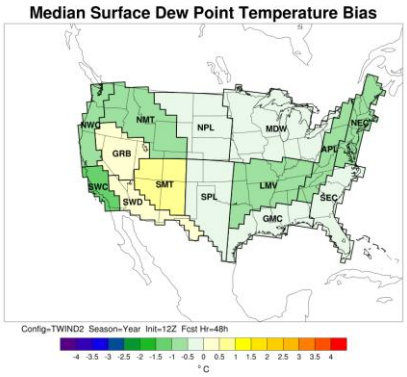

Figure 8. Regional median bias over the 5 km CONUS verification domain in 2 m AGL dew point temperature (°C) for the 12 UTC initializations, and (a) the REF configuration at 12 h lead time (b) the REF configuration at 48 h lead time, (c) the TWIND1 configuration at 12 h lead time (d) the TWIND1 configuration at 48 h lead time, (e) the TWIND2 configuration at 12 h lead time (f) the TWIND2 configuration at 48 h lead time, aggregated across the entire year of cases.

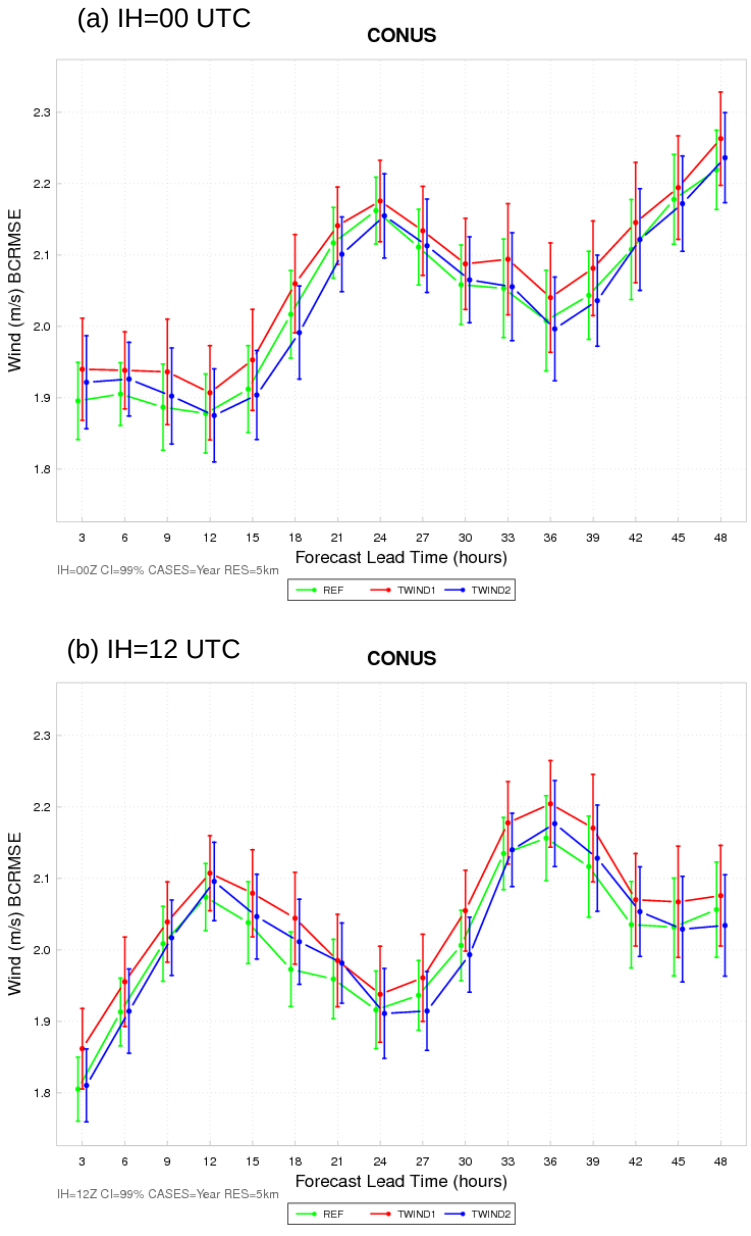

Figure 9. Time series plot of 10 m AGL wind speed (m s^{-1}) for median BCRMSE over the 5 km CONUS verification domain for (a) the 00 UTC initializations and (b) 12 UTC initializations, aggregated across the entire year of cases. The REF configuration is in green, the TWIND1 configuration in red, and the TWIND2 in blue. The vertical bars attached to the median represent the 99% CIs.

(a) Annual IH=00 UTC

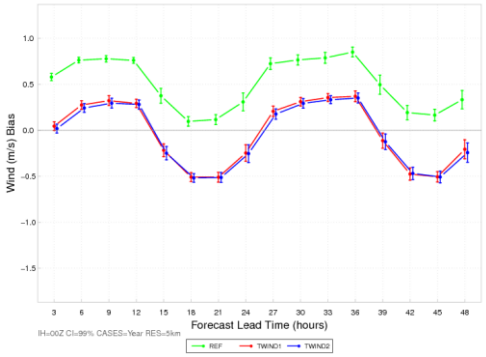

(b) Annual IH=12 UTC

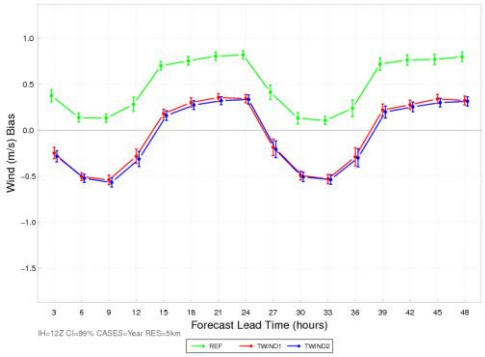

(c) Spring West IH=00 UTC

(d) Spring East IH=00 UTC

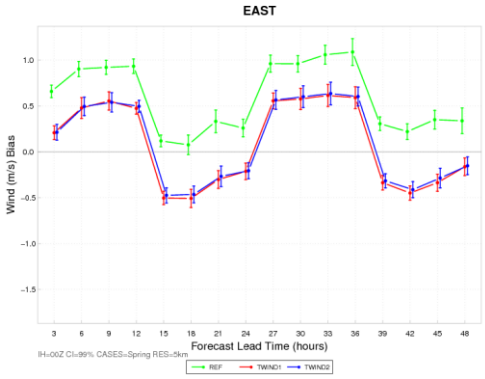

Figure 10. Time series plot of 10 m AGL wind speed (m s^{-1}) for median bias over the 5 km CONUS verification domain aggregated across the entire year of cases for the (a) 00 UTC initializations, (b) 12 UTC initializations, (c) the spring aggregation for the West verification domain, and (d) the spring aggregation for the East verification domain for the 00 UTC initializations. The REF configuration is in green, the TWIND1 configuration in red, and the TWIND2 in blue. The vertical bars attached to the median represent the 99% CIs.

Appendix A: Case list. Dates in red were not included in the verification due to missing input data.

00 UTC Initialization	12 UTC Initialization
July 2011: 1, 4, 7, 10, 13, 16, 19, 22, 25, 28, 31	July 2011: 2, 5, 8, 11, 14, **17**, 20, 23, 26, 29
August 2011: 3, 6, 9, 12, 15, 18, 21, 24, 27, 30	August 2011: 1, 4, 7, 10, 13, 16, 19, 22, 25, 28, 31
September 2011: 2, 5, 8, 11, 14, 17, 20, 23, 26, 29	September 2011: 3, 6, 9, 12, 15, 18, 21, 24, 27, 30
October 2011: 2, 5, 8, 11, 14, 17, 20, 23, 26, 29	October 2011: 3, 6, 9, 12, 15, 18, 21, 24, 27, 30
November 2011: 1, 4, 7, 10, 13, 16, 19, 22, 25, 28	November 2011: 2, 5, 8, 11, 14, 17, 20, 23, 26, 29
December 2011: 1, 4, 7, 10, 13, 16, 19, 22, 25, 28, 31	December 2011: 2, 5, 8, 11, 14, 17, 20, 23, 26, 29
January 2012: 3, 6, 9, 12, 15, 18, 21, 24, 27, 30	January 2012: 1, 4, 7, 10, 13, 16, 19, 22, 25, 28, 31
February 2012: 2, 5, 8, 11, 14, 17, 20, 23, 26,29	February 2012: 3, 6, 9, 12, 15, 18, 21, 24, 27
March 2012: 3, 6, 9, 12, 15, 18, 21, 24, 27, 30	March 2012: 1, 4, 7, 10, 13, 16, 19, 22, 25, 28, 31
April 2012: 2, 5, 8, 11, 14, 17, 20, 23, 26, 29	April 2012: 3, 6, 9, 12, 15, 18, 21, 24, 27, 30
May 2012: 2, 5, 8, 11, 14, 17, 20, 23, 26, 29	May 2012: 3, 6, 9, 12, 15, 18, 21, 24, 27, 30
June 2012: 1, 4, 7, 10, 13, 16, 19, 22, 25, 28	June 2012: 2, 5, 8, 11, 14, 17, 20, 23, 26, 29

Appendix B: A subset WRF ***namelist.input*** used in this test (for REF)

```
&time_control
run_hours                           = 48,
interval_seconds                    = 10800,
history_interval                    = 180,
frames_per_outfile                  = 1,
restart                             = .false.,
io_form_history                     = 2,
/

&domains
time_step                           = 90,
time_step_fract_num                 = 0,
time_step_fract_den                 = 1,
max_dom                             = 2,
e_we                                = 656, 1048,
e_sn                                = 464, 748,
e_vert                              = 36, 36,
num_metgrid_levels                  = 27,
dx                                  = 15000, 5000,
dy                                  = 15000, 5000,
```

p_top_requested = 5000,
interp_type = 1,
lowest_lvl_from_sfc = .false.,
lagrange_order = 1,
force_sfc_in_vinterp = 1,
zap_close_levels = 1000,
adjust_heights = .false.,
eta_levels = 1.000, 0.994, 0.982, 0.968, 0.950, 0.930, 0.908,
0.882, 0.853, 0.821, 0.788, 0.752, 0.715, 0.677,
0.637, 0.597, 0.557, 0.517, 0.477, 0.438, 0.401,
0.365, 0.330, 0.298, 0.268, 0.240, 0.214, 0.188,
0.162, 0.137, 0.114, 0.091, 0.068, 0.045, 0.022,
0.000

/

&physics
mp_physcis = 3, 3,
ra_lw_physics = 1, 1,
ra_sw_physics = 1, 1,
radt = 10, 10,
sf_sfclay_physics = 1, 1,
sf_surface_physics = 2, 2,
bl_pbl_physics = 1, 1,
topo_wind = 0, 0,
bldt = 0, 0,
cu_physics = 1, 0,
cudt = 5,
surface_input_source = 1,
num_soil_layers = 4,
mp_zero_out = 2,
/

&dynamics
diff_6th_opt = 0, 0,
diff_6th_factor = 0.12, 0.12,
w_damping = 1,
diff_opt = 1,
km_opt = 4,
damp_opt = 0,
zdamp = 5000., 5000.,

```
base_temp               = 290.,
dampcoef                = 0.01, 0.01,
khdif                   = 0, 0,
kvdif                   = 0, 0,
non_hydrostatic         =.true., .true.,
scalar_adv_opt          = 1, 1,
moist_adv_opt           = 1, 1,
/

&bdy_control
spec_bdy_width          = 5,
spec_zone               = 1,
relax_zone              = 4,
specified               = .true., .false.,
nested                  = .false., .true.,
/
```